J Mol Model (2013) 19:825–832
DOI 10.1007/s00894-012-1609-7

ORIGINAL PAPER

Steered molecular dynamics simulation of the binding of the β2 and β3 regions in domain-swapped human cystatin C dimer

Jianwei He · Linan Xu · Shuo Zhang · Jing Guan · Manli Shen · Hui Li · Youtao Song

Received: 14 February 2012 / Accepted: 25 September 2012 / Published online: 12 October 2012

Abstract The crystal structure of the human cystatin C (hCC) dimer revealed that a stable twofold-symmetric dimer was formed via 3D domain swapping. Domain swapping with the need for near-complete unfolding has been proposed as a possible route for amyloid fibril initiation. Thus, the interesting interactions that occur between the two molecules may be important for the further aggregation of the protein. In this work, we performed steered molecular dynamics (SMD) simulations to investigate the dissociation of the β2 and β3 strands in the hCC dimer. The energy changes observed during the SMD simulations showed that electrostatic interactions were the dominant interactions involved in stabilizing the two parts of the dimer during the early stages of SMD simulation, whereas van der Waals (VDW) interactions and electrostatic interactions were equally matched during the latter stages. Furthermore, our data indicated that the two parts of the dimer are stabilized by intermolecular hydrogen bonds among the residues Arg51 (β2), Gln48 (β2), Asp65 (β3), and Glu67 (β3), salt bridges among the residues Arg53 (β2), Arg51 (β2), and Asp65 (β3), and VDW interactions among the residues Gln48 (β2), Arg51 (β2), Glu67 (β3), Asp65 (β3), Phe63 (β3), and Asn61 (β3). The residues Gln48 (β2), Arg51 (β2), Asp65 (β3) and Glu67 (β3) appear to be crucial, as they play important roles in both electrostatic and VDW interactions. Thus, the present study determined the key residues involved in the stabilization of the domain-swapped dimer structure, and also provided molecular-level insights into the dissociation process of the hCC dimer.

Keywords Human cystatin C · Steered molecular dynamics · Domain swapping · Dimer

J. He · L. Xu · S. Zhang · J. Guan · M. Shen · H. Li · Y. Song
Province Key Laboratory of Animal Resource and Epidemic Disease Prevention, College of Life Science, Liaoning University, Shenyang 110036, China

M. Shen · Y. Song (✉)
School of Environmental Science, Liaoning University, Shenyang 110036, China
e-mail: youtaos@gmail.com

Introduction

More than 20 proteins or their proteolytic products are now known to form amyloid fibrils in human proteins [1]. Human cystatin C amyloid angiopathy (HCCAA) is a dominantly inherited disorder characterized by tissue deposition of amyloid fibrils in blood vessels that leads to recurrent hemorrhagic stroke [2]. In addition, it has been reported that human cystatin C (hCC) can bind to Aβ peptide and affect its amyloid fibril formation in Alzheimer's disease [3]. The native structure of each cystatin molecule consists of a five-stranded antiparallel β-sheet wrapped around a long central helix. In the morbid state, the original monomer exchanges its β1-(α)-β2 domain with the same part of the other monomer, forming a dimeric structure which is the basic unit of pathogenic amyloid fibrils [4]. Such large-scale structural rearrangements must involve partial unfolding of the original native structure of the monomer and refolding of the hybrid structure. Recently, an analogous domain-swapping process, propagating in an open-ended fashion, has been suggested to be the fundamental mechanism of HCC oligomerization in the context of amyloid fibril formation [5], so domain swapping is pivotal for structural stabilization en route to oligomerization. Consequently, the interesting interactions between the two molecules constituting the

domain-swapped dimer are of great importance, not only for the dimerization reaction but also for the subsequent oligomerization process, since structural rearrangement within the dimer is certainly a prerequisite for oligomer formation.

According to the 3D structure of the hCC dimer, one monomer binds to the other through two major interaction regions: a peripheral region formed by the appendant structure (AS) and part of helix β2, and a central region formed by β2 and β3 [6, 7]. Our previous molecular dynamics studies showed that AS plays an important role in the unfolding of the monomer, and a distorted AS was favorable to intermolecular interactions between the two cystatin monomers [8]. Further studies suggested that the "clothespin" structures formed by interactions between AS and the β2 helix were responsible for stabilizing the structure of the domain-swapped dimer [9]. On the other hand, Rodziewicz-Motowidło et al. reported that the point mutation V57N in the L1 loop in the β1-L1-β2 fragment of hCC gave rise to a much broader L1 loop, leading to easier conversion to the more stable dimeric form than seen for the other hCC mutants [10]. However, a close study of the intermolecular interactions between β2 and β3 within the dimer is yet to be performed. Structurally, both of the two β-strands are located within the central region of the dimer, which leads us to believe that they should play an important role in stabilizing the whole dimer structure.

Classical molecular dynamics (MD) methods are mainly applied to simulate systems under equilibrium conditions [11]; applying these methods to nonequilibrium systems (such as those undergoing domain swapping) requires immense computational power and is extremely time consuming. In the work described in this paper, we utilized steered molecular dynamics (SMD)—which was used to study ligand–receptor or protein–protein unbinding through application of the time-dependent external forces—to obtain the process details of domain-swapped cystatin dimerization by studying the reverse process [12]. Moreover, we believed that SMD simulation studies on the dissociation process would provide valuable information on the structural rearrangement that occurs within the dimer.

In order to study the intermolecular binding of the β2 and β3 regions in the domain-swapped hCC dimer, the β2 region was pulled away from the β3 region at a constant velocity. The conformational changes that occur during the unbinding process were explored by investigating crucial interactions among activated residues in both the β2 and β3 strands. By comparing the results for interaction energy, hydrogen bonds, salt bridges, and hydrophobic interactions, it was possible to identify the key residues involved in the pivotal interactions between the two monomers. The information obtained from these results may aid our understanding of the closed domain-swapping mechanism of the hCC dimer as well as the propagated domain-swapping mechanism associated with oligomerization.

Methods

Model construction

The model of the hCC dimer molecule used in our study was constructed according to the X-ray crystal structure and coordinates of the human cystatin C dimer (PDB ID: 1TIJ), which was obtained from the RCSB Protein Data Bank [6].

MD and SMD simulations

The MD simulation was performed using the Gromacs 4.0 program [13] at the Computer Center of Liaoning University (CCLU) on a dual-core Pentium 2.8G processor in a Linux cluster. GROMOS96 43a1 [14] force-field parameters were used in all of the simulations performed in this study. Integration time steps of 2 fs were used throughout the whole simulation. The short-range nonbonded interactions were defined as van der Waals and electrostatic interactions between particles within 0.9 nm. Long-range electrostatic interactions were calculated with the particle mesh Ewald (PME) method [15] with a maximum FFT grid spacing of 0.12 nm and cubic interpolation. Periodic boundary conditions were activated in the simulations. Bonds containing hydrogen atoms were constrained using the SHAKE algorithm with a relative tolerance of 10^{-5} Å. The dimeric hCC model was solvated in a water box containing 39,110 SPC216 water molecules [16] and neutralized by adding three Cl^- counterions. The volume of the cubic box was $20\times20\times20$ nm^3. The solvated and neutralized systems were energy-minimized for 20 ps. Afterwards, the backbone atoms of the structure were fixed while the side chains and solvent were allowed to move under minimal restraint for a further 10 ps, followed by completely unrestrained equilibration for 12 ps, at a constant temperature of 300 K and a pressure of 1 atm, within a water box, using periodic boundary conditions in the NPT ensemble. Following equilibration, the production run was carried out over 3 ns with the temperature kept constant at 300 K, pH 7. In all simulations, the temperature was maintained close to the intended values by weakly coupling to an external temperature bath with a coupling constant of 0.1 ps. The protein and the rest of the system were coupled separately to the temperature bath.

Afterward, SMD simulations with constant velocity were performed. In this process, keeping the center of mass of the β3 region (residues Gly59 to Gly69) fixed, external steering forces were applied to the reference

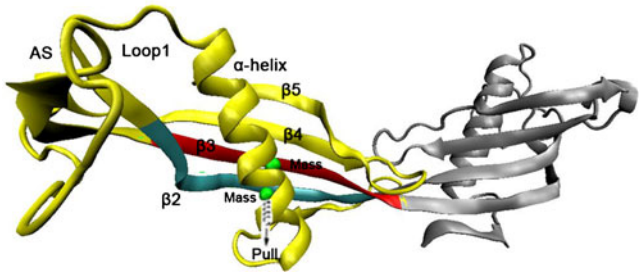

Fig. 1 Ribbon representation of the hCC dimer. The pulling region of β2 and the fixed region of β3 are highlighted in *cyan* and *red*, respectively. The *green balls* show the centers of mass of the Cα atoms, to which fixed and harmonic potentials were assigned, and the *spring with arrow* shows the direction of movement of β2 from β3 in the SMD simulations

point (the center of mass of the β2 region, i.e., residues Arg45 to Val57) to pull the β2 domain along the predefined direction (Fig. 1). During the SMD simulations, the force was only applied along the pulling direction. Based on the 3D structure of the hCC dimer and the hypothetical domain swapping mechanism, the pulling direction in the system was assigned to all pairs contributing hydrogen bonds between the pull regions to achieve effective separation of β2. The trajectories were saved every 0.5 ps, and steering forces were recorded every 10 fs. Three trajectories along the each pathway were recorded.

Analysis of the trajectories

The secondary structure of the protein was determined using the DSSP program [17]. Visual Molecular Dynamics (VMD) software [18] and the LigPlot program [19] with appropriately developed original scripts were used for system visualization and analysis. Root mean square deviations (RMSD) were calculated for all α-carbon atoms, with the first frame of the trajectory used as the reference.

Results and discussion

Determination of the pulling velocity and spring constant

To equilibrate the interaction regions before performing the SMD simulations, a 3 ns MD simulation of the fully solvated hCC dimer was carried out at pH 7.0 and 300 K. The root-mean-square deviation (RMSD) profile indicated that the conformation of the protein equilibrated a short time after the beginning of the simulation, and the RMSD values were generally stabilized at 0.40 nm for all α-carbon atoms. The stable structure of the protein provides a reasonable starting point for the subsequent SMD simulations.

In constant velocity SMD (cv-SMD), the value of the spring force varies significantly, depending on the pulling velocity and spring constant. A previous study has shown that a higher pulling velocity leads to disequilibrium, and may introduce errors into the simulation results [20]. To avoid inducing experimental errors in the system, and in accordance with atomic force microscopy (AFM) experiments, the pulling velocity should be as small as possible [21]. To choose a suitable velocity for the hCC dimer system, we carried out eleven simulations, each employing a different pulling velocity ranging from 0.003 nm/ps to 0.06 nm/ps. Figure 2a summarizes the rupture forces caused by different pulling velocities. There was an obvious linear dependency between rupture force and pulling velocity when the velocity

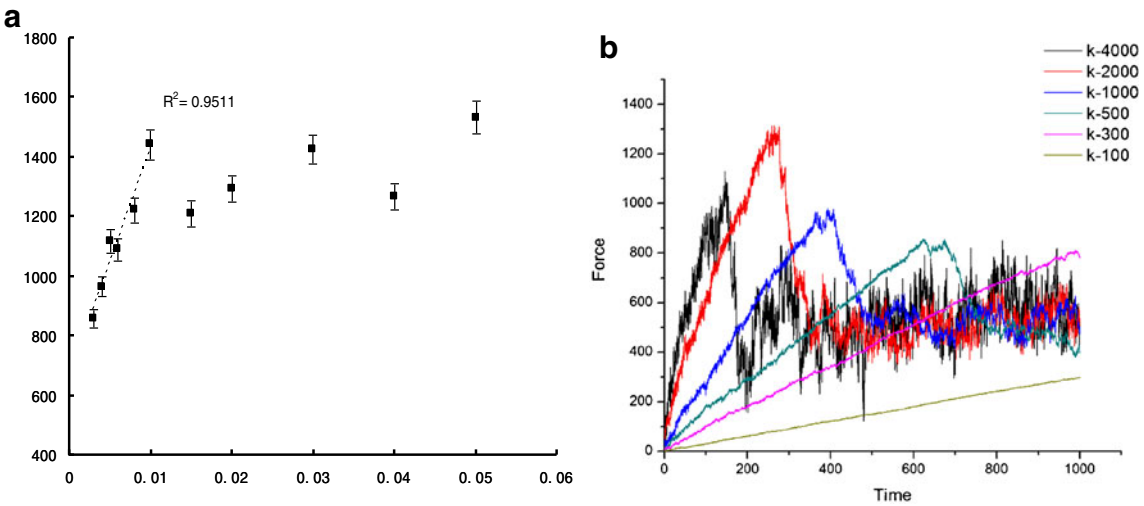

Fig. 2 **a** Computed rupture forces as a function of pulling velocity (V_{pull}). The *error bars* give estimated uncertainties. The *dashed line* shows a linear fit to the computed forces for V_{pull} <0.01 nm/ps. **b** Influence of the spring constant on the steering force of the dimer

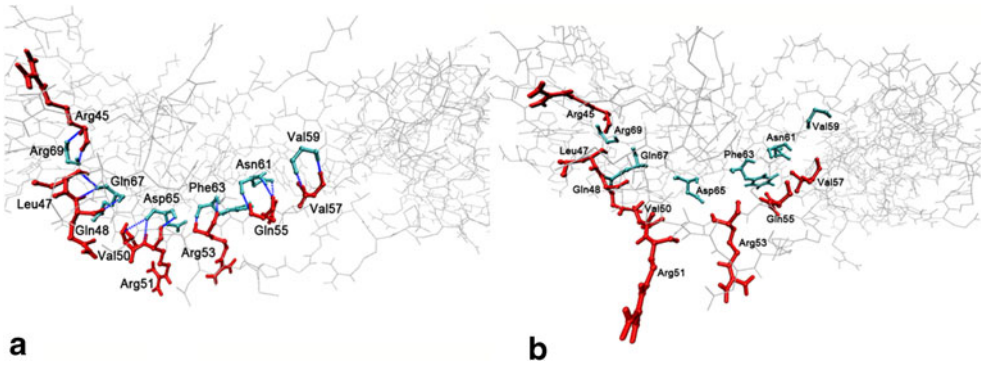

Fig. 3 Changes observed in the structures of the β2 and β3 regions after SMD simulation. **a** The positions of the residues in the original structure that are linked by hydrogen bonds. **b** The positions of these related residues after SMD simulation. Hydrogen bonds are represented by *dashed blue lines*; other residues are presented by *thin gray lines*

was <0.01 nm/ps. In the subsequent SMD simulations, the lowest velocity of 0.003 nm/ps was chosen so that the external harmonic potential did not appear to have any obvious influence on the structure of the β2 fragment.

When choosing the spring constant to use in the SMD simulation, two major factors need to be considered; the spring constant must be high enough to enable the local unbinding potential to be determined, but it must not be so high that the measured force is masked by background noise [21]. To choose an appropriate spring constant, we performed six simulations with various spring constants ranging from 100 to 4,000 $kJmol^{-1}nm^{-2}$ (Fig. 2b). The results showed that under the same pulling velocity, the smaller the spring constant, the later the occurrence of the peak force, and the more distinct the peak. Spring constants of 4,000, 2,000, and 1,000 $kJmol^{-1}nm^{-2}$ produced obvious fluctuations in the force curve across the whole simulation. In contrast, spring constants of 100 and 300 $kJmol^{-1}nm^{-2}$ failed to produce sufficient fluctuations in peak intensity, which suggests that these spring constants are not enough to ensure the validity of the stiff-spring approximation for the guiding potential (Fig. 2b). A spring constant of 500 $kJmol^{-1}nm^{-2}$ produced measurable and reliable peak fluctuations with minimal background noise (Fig. 2b), and was therefore chosen for subsequent SMD simulations.

Conformational changes of the hCC dimer

According to the RMSD values observed in the SMD simulations, obvious conformational changes occur in the hCC dimer during the unbinding process (data not shown). Figure 3a shows the original structure of the hCC dimer after 3 ns of MD simulation. There are 15 hydrogen bonds (blue) from the residues Arg45, Leu47, Gln48, Val50, Arg51, Arg53, Gln55, and Val57 located on the β2 fragment (red) to Arg69, Gln67, Asp65, Phe63, Asn61, and Val59 located on the β3 fragment (cyan) of the other monomer. This hydrogen bond network is responsible for the structural stability of the hCC dimer. After 1 ns of SMD simulation, the β2 fragment apparently shifts from its original location onto the β3 fragment side (Fig. 3b). The distances between the center of mass of the β2 fragment and that of the β3 fragment before and after pulling were 0.23 nm and 1.47 nm, respectively. Because the pulling direction applied to the system was chosen such that effective separation of

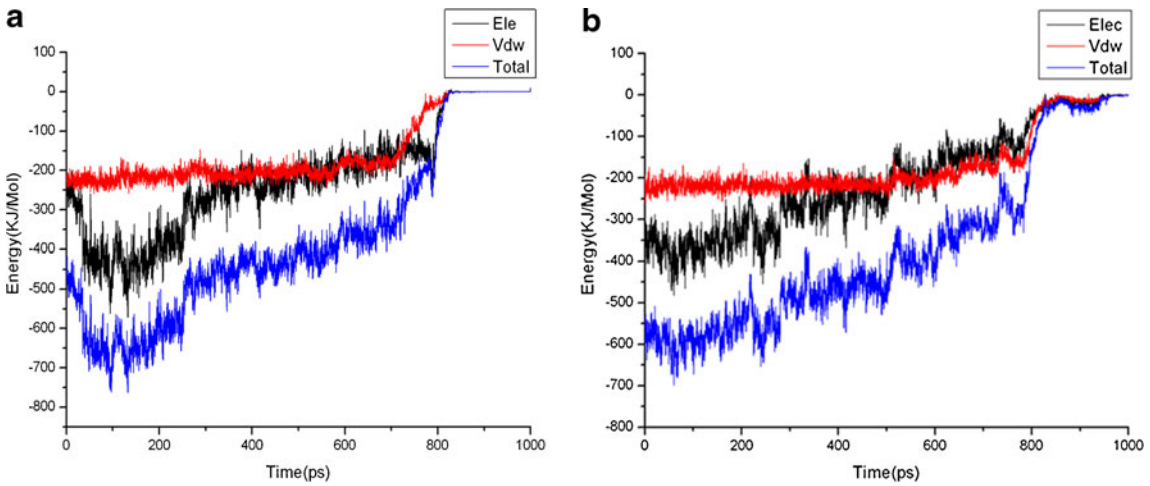

Fig. 4 Time dependence of the interaction energy between the β2 and β3 regions during the SMD simulation. **a** Pulling β2 away from the β3 fragment on the left side of the hCC dimer; **b** pulling β2 from the β3 fragment on the right side of the hCC dimer

β2 was achieved, all 15 of the hydrogen bonds between residues in β2 and those in β3 regions disappeared (Fig. 3b). This indicated that β2 was completely pulled away from β3 and that the hydrogen-bonded network was clearly disrupted during this process.

Energy analysis of the dissociation process

The dissociation of β2 from β3 is a dynamic procedure that is determined by the lowest free-energy state. In the non-equilibrium SMD simulations, the changes in interaction energy between the pulling regions were taken into account during the pulling progress. As shown in Fig. 4a, the starting point for the curve is the stable state with the lowest free energy. After the first point, the system enters a nonequilibrium state because of the effect of the force applied. The curve of the interaction energy decreases over time, which indicates that there is a strong interaction between the β2 and β3 fragments during the dynamic procedure. The total energy reaches a minimum at about 100 ps, which suggests that the interaction between the two β fragments increases to the maximum, when the energy reaches the lowest value. It is also clear that electrostatic interactions are dominant during the early stages of SMD simulation (0~300 ps), whereas both electrostatic interactions and VDW interactions are equally matched during the latter stages (300~800 ps).

Table 1 Residue pairs involved in hydrogen bonding

Residue in β2	Residue in β3
Arg51(N)	Asp65(O)
Arg51(O)	Asp65(N)
Arg53(N)	Phe63(O)
Arg53(O)	Phe63(N)
Gln48(N)	Glu67(O)
Gln48(O)	Glu67(N)

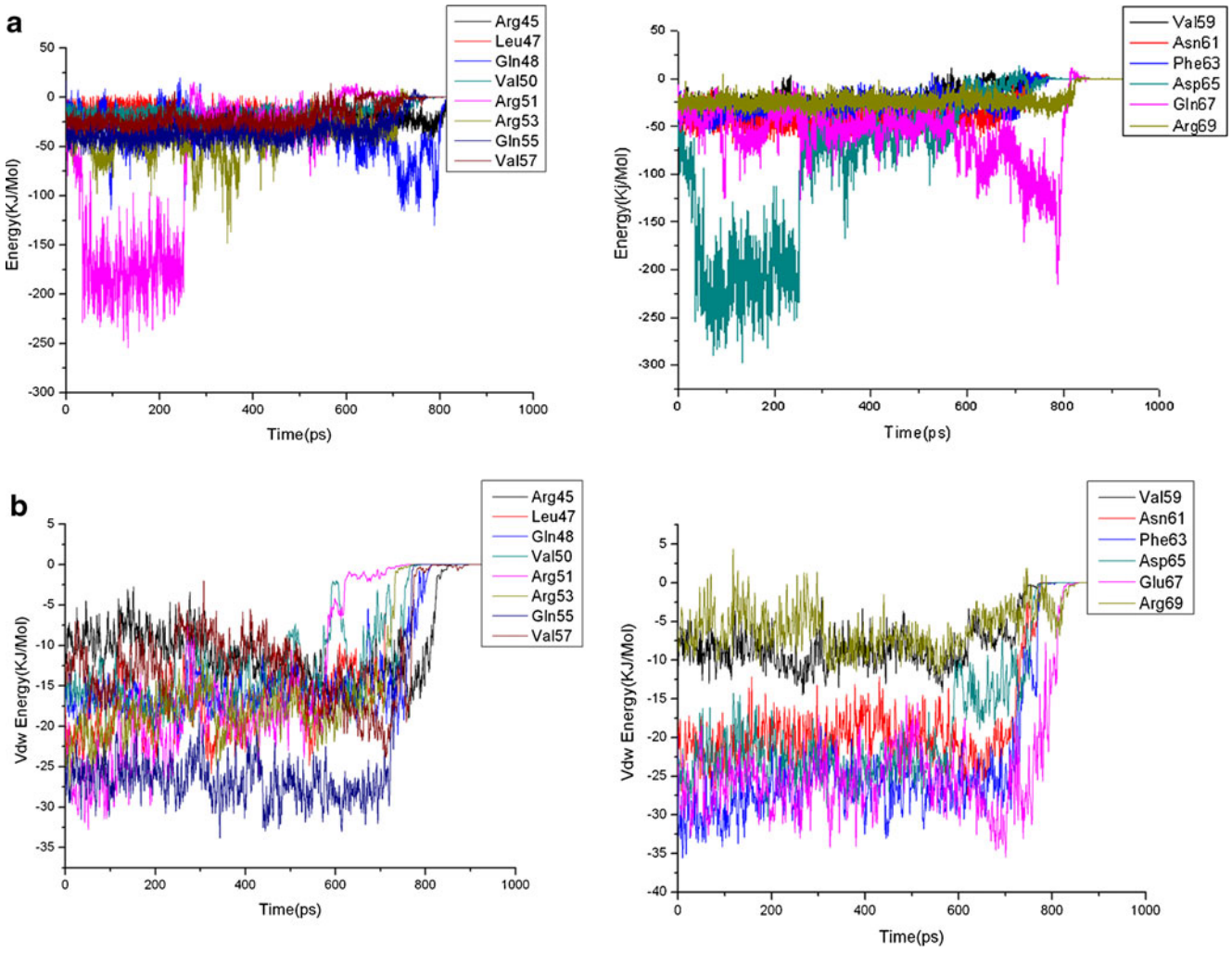

Fig. 5 Plots showing the time dependence of the interaction energy for various residues in the β2 and β3 regions during SMD simulation. **a** Electrostatic interaction energies; **b** VDW interaction energies. Residues in the β2 fragment are shown on the *left* and residues in the β3 fragment are shown on the *right*

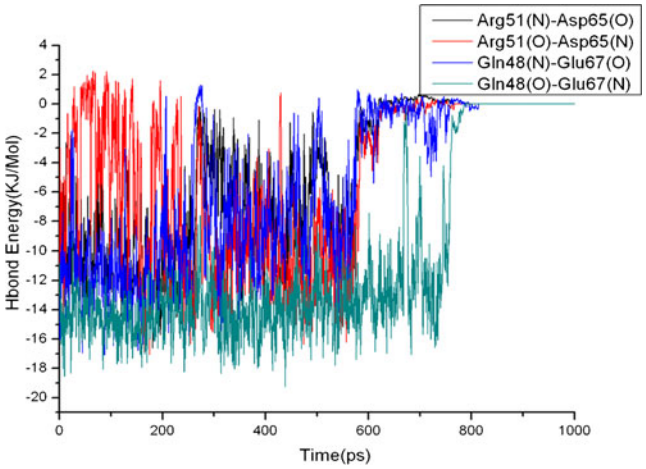

Fig. 6 Energy analyses of four hydrogen bonds during SMD simulation

After 800 ps, the energy curve quickly drops to zero, which suggests that the β2 fragment has completely dissociated from the β3 region. In addition, an analysis of the interaction energy for the pulling region on the right side of the hCC dimer gave similar results to a similar analysis performed for the left side (Fig. 4b), which confirms that the structure of the hCC dimer in these regions is symmetric [4].

To investigate the role of the residues linked by hydrogen bonds in the pulling region, we analyzed the electrostatic interactions and VDW interactions among residues in the hydrogen-bonded network present in the β2 and β3 regions. As shown in Fig. 5a, deep valleys in the interaction curves indicated that the most important electrostatic interactions between the β2 and β3 fragments are associated with residues Arg51 (β2) and Asp65 (β3) in the first phase (0~300 ps), Arg53 (β2) and Asp65 (β3) in the second phase (300~600 ps), and Gln48 (β2) and Gln67 (β3) in the third phase (600~800 ps). The relatively flat interaction energy curves of other residues suggest that they are less important. Furthermore, Fig. 5b shows that several important VDW interactions that occurred between the β2 and β3 fragments during the SMD simulation were associated with residues Gln48 (β2), Glu67 (β3), Asp65 (β3), Phe63 (β3), and Asn61 (β3).

Analysis of hydrogen-bonding status during the dissociation process

Hydrogen bonds are the most abundant type of non-covalent interaction and are important for stabilizing protein structures. Previous analysis of the hCC dimer crystal structure revealed extensive electrostatic interactions between the β2 and β3 regions [6]. We therefore determined the interchain hydrogen bonds present during the dissociation process (Table 1) and compared the residue pairs involved in these hydrogen bonds with our results for the residues associated with electrostatic interactions between β2 and β3. The comparison indicated that the hydrogen bonds Arg51(N)–Asp65(O), Arg51(O)–Asp65(N), Gln48(N)–Glu67(O), and Gln48(O)–Glu67(N) correlated exactly with the residues involved in electrostatic interactions (Fig. 5a). However, the hydrogen bonds Arg53(N)–Phe63(O) and Arg53(O)–Phe63(N) did not correlate with the results for the electrostatic interactions (based on electrostatic energy, Arg53 should be linked to Asp65), suggesting that these two hydrogen bonds are very weak and that Arg53 interacts with Asp65 through other types of electrostatic interaction. To estimate the strength of these hydrogen bonds, we further analyzed the interaction energy of the four important hydrogen bonds listed above (Fig. 6). The hydrogen bonds Arg51(N)–Asp65(O), Arg51(O)–Asp65(N), Gln48(N)–Glu67(O), and Gln48(O)–Glu67(N) were not broken until 600 ps and 800 ps into the SMD simulation, respectively. This suggests that hydrogen bonds were not the dominant electrostatic interactions during the early stages of SMD simulation (0~600 ps), but the hydrogen bond Gln48(O)–Glu67(N) played an important role in the intermolecular interaction during the middle stages of SMD simulation (600~800 ps).

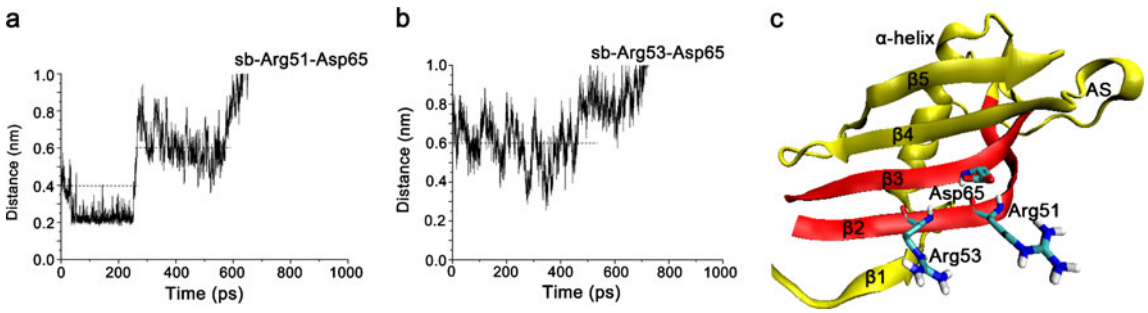

Fig. 7 The salt-bridge distances of Arg51–Asp65 (**a**) and Arg53–Asp65 (**b**) as a function of SMD simulation time

Analysis of salt-bridge formation during the dissociation process

Among the various types of electrostatic interaction, salt bridges play a major role in determining the tensile strength of protein–protein interactions. Thus, we evaluated the electrostatic interactions by calculating the distances between all charged groups in the pulling region. Based upon previously published data, if the distance between two oppositely charged residues was within 0.4 nm it was defined as a strong salt bridge, and if the distance was within 0.6 nm it was considered a weak salt bridge [22]. Figure 7 summarizes the most important salt bridges that formed during the dissociation process. These salt bridges occurred between Arg53 (β2), Arg51 (β2), and Asp65 (β3), and were directly connected to parts of the strands close to the loop site, which was important for stabilizing the dimer structure. The salt bridges seemed to be relatively stable because of the low-dielectric environment in the interior of β2 and β3. When considered in parallel with the interaction energies of related residues (Fig. 5b), these results indicate that Arg51–Asp65 is a strong salt bridge, while Arg53–Asp65 is a weak one. In addition, the relationship between salt-bridge distance and SMD simulation time suggested that these two salt bridges could be the dominant electrostatic interactions during the early stages of SMD simulation (0~600 ps).

Conclusions

Human cystatin C (hCC) was the first disease-causing amyloidogenic protein whose oligomerization was shown to be dependent on domain swapping [4, 23]. Recent experiments on hCC have shown that prevention of domain swapping inhibits amyloid fibrils by up to 80 % [24]. However, the exact mechanism of the dynamic process of domain swapping performed by unfolded cystatin monomers is yet to be elucidated. Based on the 3D structure of the hCC dimer, interactions between the monomers occur through two major interaction regions: a side region formed by the AS and part of helix β2, and a central region formed by the β3 and β2 strands [4, 7].

In this work, SMD simulations of the hCC dimer aimed at investigating the dissociation of β2 from β3 were performed for the first time. The results showed that the interactions between the β2 and β3 regions during the SMD simulations could be divided into three stages during 1 ns of SMD simulation: (1) 0~300 ps, electrostatic interactions (strong salt bridges) were dominant; (2) 300~600 ps, electrostatic interactions (weak salt bridges) and VDW interactions were equally matched; (3) 600~800 ps, electrostatic interactions (hydrogen bonds) and VDW interactions were equally matched. Further study indicated that the intermolecular hydrogen bonds among the residues Arg51 (β2), Gln48 (β2), Asp65 (β3), and Glu67 (β3), the salt bridges among the residues Arg53 (β2), Arg51 (β2), and Asp65, and VDW interactions among the residues Gln48 (β2), Glu67 (β3), Asp65 (β3), Phe63 (β3), and Asn61 (β3) together contribute to stabilizing the two parts of the dimeric structure. The residues Gln48 (β2), Arg51 (β2), Asp65 (β3), and Glu67 (β3) were found to be particularly important, as they played important roles in both the electrostatic and VDW interactions. Combining our SMD simulation results, the overall conclusion was that the interactions between the two symmetric β2 and β3 segments of the two molecules and the key residues involved in these interactions play important roles in increasing the binding affinity in this complex system and binding the two molecules within it easily and tightly, although these interactions or key residues are unlikely to directly trigger the domain-swapping process.

Analyses of our simulation results provided more detailed information on the formation of the domain-swapped hCC dimer. Moreover, the results of this study also provide important clues about the propagated domain-swapping mechanism, as the dissociation of the hCC dimer is a prerequisite for this mechanism. In fact, the actual domain swapping may not simply be the reverse of the hCC dimer unbinding process, so it will be necessary to screen a series of related mutants to verify the hypothesis we have developed based on SMD simulations and biological experiments. Nevertheless, these findings will provide new insights into the mechanism of hCC domain swapping, and should prove helpful when attempting to find methods of preventing hCC amyloid fibril formation.

Acknowledgments This work was supported by grants from the National Natural Science Foundation of China (no. 30970152) and was partially sponsored by the Scientific Research Foundation for Returned Overseas Chinese Scholars (no. 2010-1561), State Education Ministry.

References

1. Revesz T, Ghiso J, Lashley T, Plant G, Rostagno A, Frangione B, Holton JL (2003) Cerebral amyloid angiopathies: a pathologic, biochemical, and genetic view. J Neuropathol Exp Neurol 62 (9):885–898
2. Sanders A, Jeremy Craven C, Higgins LD, Giannini S, Conroy MJ, Hounslow AM, Waltho JP, Staniforth RA (2004) Cystatin forms a tetramer through structural rearrangement of domain-swapped dimers prior to amyloidogenesis. J Mol Biol 336(1):165–178
3. Kaeser SA, Herzig MC, Coomaraswamy J, Kilger E, Selenica ML, Winkler DT, Staufenbiel M, Levy E, Grubb A, Jucker M (2007) Cystatin C modulates cerebral beta-amyloidosis. Nat Genet 39 (12):1437–1439
4. Janowski R, Kozak M, Jankowska E, Grzonka Z, Grubb A, Abrahamson M, Jaskolski M (2001) Human cystatin C, an amyloidogenic protein, dimerizes through three-dimensional domain swapping. Nat Struct Biol 8(4):316–320

5. Wahlbom M, Wang X, Lindstrom V, Carlemalm E, Jaskolski M, Grubb A (2007) Fibrillogenic oligomers of human cystatin C are formed by propagated domain swapping. J Biol Chem 282 (25):18318–18326
6. Janowski R, Kozak M, Abrahamson M, Grubb A, Jaskolski M (2005) 3D domain-swapped human cystatin C with amyloidlike intermolecular beta-sheets. Proteins 61(3):570–578
7. Schlunegger MP, Bennett MJ, Eisenberg D (1997) Oligomer formation by 3D domain swapping: a model for protein assembly and misassembly. Adv Protein Chem 50:61–122
8. Yu Y, Liu X, He J, Zhang M, Li H, Wei D, Song Y (2012) Appendant structure plays an important role in amyloidogenic cystatin dimerization prior to domain swapping. J Biomol Struct Dyn 30:102–12
9. Shen M, Guan J, Xu L, Yu Y, He J, Jones G, Y. S (2012) Steered molecular dynamics simulations on the binding of the appendant structure and helix-β2 in domain-swapped human cystatin C dimer. J Biomol Struct Dyn 30(6):652–61
10. Rodziewicz-Motowidlo S, Iwaszkiewicz J, Sosnowska R, Czaplewska P, Sobolewski E, Szymanska A, Stachowiak K, Liwo A (2009) The role of the Val57 amino-acid residue in the hinge loop of the human cystatin C. Conformational studies of the beta2-L1-beta3 segments of wild-type human cystatin C and its mutants. Biopolymers 91(5):373–383
11. Zhang B, Tan VB, Lim KM, Tay TE (2006) Molecular dynamics simulations on the inhibition of cyclin-dependent kinases 2 and 5 in the presence of activators. J Comput Aided Mol Des 20(6):395–404
12. Orzechows M, Cieplak P (2005) Application of steered molecular dynamics (SMD) to study DNA–drug complexes and probing helical propensity of amino acids. J Phys Condens Matter 17:1627–1640
13. Hess B, Kutzner C, Van Der Spoel D, Lindahl E (2008) GROMACS 4: algorithms for highly efficient, load-balanced, and scalable molecular simulation. J Chem Theory Comput 4 (3):435–447
14. Bonvin AM (2006) Flexible protein-protein docking. Curr Opin Struct Biol 16(2):194–200
15. Darden T, York D, Pedersen L (1993) Particle mesh Ewald: an Nlog(N) method for Ewald sums in large systems. J Chem Phys 98:10089–10092
16. Berendsen HJC, Postma JPM, van Gunsteren WF, Hermans J (1981) Interaction models for water in relation to protein hydration. In: Pullman B (ed) Intermolecular forces. Reidel, Dordrecht, pp 331–342
17. Kabsch W, Sander C (1983) Dictionary of protein secondary structure: pattern recognition of hydrogen-bonded and geometrical features. Biopolymers 22(12):2577–2637
18. Humphrey W, Dalke A, Schulten K (1996) VMD: visual molecular dynamics. J Mol Graph 14(1):33–38, 27–38
19. Wallace AC, Laskowski RA, Thornton JM (1995) LIGPLOT: a program to generate schematic diagrams of protein–ligand interactions. Protein Eng 8(2):127–134
20. Isralewitz B, Gao M, Schulten K (2001) Steered molecular dynamics and mechanical functions of proteins. Curr Opin Struct Biol 11(2):224–230
21. Zhang J, Zheng Q, Zhang H (2010) Unbinding of glucose from human pulmonary surfactant protein D studied by steered molecular dynamics simulations. Chem Phys Lett 484: 338–343
22. Tiberti M, Papaleo E (2011) Dynamic properties of extremophilic subtilisin-like serine-proteases. J Struct Biol 174(1):69–83
23. Staniforth RA, Giannini S, Higgins LD, Conroy MJ, Hounslow AM, Jerala R, Craven CJ, Waltho JP (2001) Three-dimensional domain swapping in the folded and molten-globule states of cystatins, an amyloid-forming structural superfamily. EMBO J 20 (17):4774–4781
24. Nilsson M, Wang X, Rodziewicz-Motowidlo S, Janowski R, Lindstrom V, Onnerfjord P, Westermark G, Grzonka Z, Jaskolski M, Grubb A (2004) Prevention of domain swapping inhibits dimerization and amyloid fibril formation of cystatin C: use of engineered disulfide bridges, antibodies, and carboxymethylpapain to stabilize the monomeric form of cystatin C. J Biol Chem 279(23):24236–24245